Cells and Materials

Volume 7 | Number 2 Article 5

1997

Detachment of Human Endothelial Cells Under Flow From Wettability Gradient Surfaces with Different Functional Groups

T. G. Ruardy
University of Groningen

H. E. Moorlag
University of Groningen

J. M. Schakenraad
University of Groningen

H. C. van der Mei
University of Groningen

H. J. Busscher
University of Groningen

Cells and Materials Vol. 7, No. 2, 1997 (Pages 123-133) 1051-6794/97$5.00+.25
Scanning Microscopy International, Chicago (AMF O'Hare), IL 60666 USA

DETACHMENT OF HUMAN ENDOTHELIAL CELLS UNDER FLOW FROM WETTABILITY GRADIENT SURFACES WITH DIFFERENT FUNCTIONAL GROUPS

T.G. Ruardy[1], H.E. Moorlag[1], J.M. Schakenraad[2], H.C. van der Mei[1], and H.J. Busscher[1*]

[1]Laboratory for Materia Technica, University of Groningen, Groningen, The Netherlands
[2]Department of Artificial Organs, Division Biomaterials, University of Groningen, Groningen, The Netherlands

(Received for publication March 26, 1997 and in revised form June 23, 1997)

Abstract

In this study, the position bound adhesion, spreading and detachment under flow of human umbilical cord endothelial cells (HUVEC) was studied on a dichlorodimethylsilane (DDS), dimethylocta-decylchlorosilane (DOCS) and tridecafluor-1,1,2,2-tetrahydrooctyl-1-dimethylchlorosilane (TFCS) wettability gradient on glass. Gradient surfaces were prepared by the diffusion method and characterized by the Wilhelmy plate technique for their wettability and by X-ray photoelectron spectroscopy (XPS) for their chemical composition. Quantitative analysis of the cellular response on the wettability gradient surfaces showed that the position bound cellular response was influenced by wettability for each type of gradient in a different way. On DDS-wettability gradients, cells withstood flow best on hydrophilic regions of the gradient with advancing water contact angles below 25 degrees while on TFCS-wettability gradients this inversal point was located on regions of the gradient with advancing water contact angles around 65 degrees. After the onset of flow, cells detached from the DOCS surface, but remained adhering in low numbers irrespective of the position bound wettability. This paper confirms that cells have unfavourable interactions with hydrophobic, immobile surfaces, like adsorbed DDS on glass. However, if the hydrophobicity is created by more mobile, relatively long chain groups, possibly yielding incomplete surface coverage due to their mobility, favourable interactions may also occur on more hydrophobic surfaces.

Key Words: Endothelial cells, adhesion, wettability gradient, flow.

*Address for correspondence:
H.J. Busscher
Laboratory for Materia Technica
University of Groningen, Bloemsingel 10,
9712 KZ Groningen, The Netherlands
Telephone Number: +31 50 363 3140
FAX Number: +31 50 363 3159
e-mail: h.j.busscher@med.rug.nl

Introduction

Successful incorporation of a biomaterials implant into the human body, like for instance vascular grafts, artificial heart valves, skin or joint prostheses, depends for a major part on the surface chemistry (Kishida *et al.*, 1991), charge (Davies, 1988), roughness (Chehroudi *et al.*, 1989) and wettability (Van Wachem *et al.*, 1985) of the implants surface, together with accompanying specific protein exchange interactions (Groth *et al.*, 1994; Steele *et al.*, 1991). The final interaction between a biomaterials surface and living tissue is determined by an interplay of all surface properties involved and the contribution of a single property is hard to determine. *In vitro* and *in vivo* studies have attempted to establish the influence of wettability or surface free energy on cellular adhesion and spreading (Schakenraad *et al.*, 1986; 1987; Baier *et al.*, 1985) on a series of biomaterials, but rigorous interpretation of the results are hampered by the fact that not only the wettability of the biomaterials used varies, but much more so, also the specific surface chemistry of the materials.

A minimal variation in specific surface chemistry along with a sizeable variation in wettability can be accomplished by preparation of a series of surface modified substrata (Bruil *et al.*, 1994) or the use of so-called wettability gradient surfaces (Elwing *et al.*, 1987; Gölander and Pitt, 1990). A main feature of a wettability gradient surface is that a whole range of continuously changing physico-chemical properties is present along the length of one single sample. For biomaterials research, gradient surfaces offer exciting options because 1) an extensive variation in specific surface chemistry is avoided and 2) experiments can be done e.g. over the entire wettability spectrum using only one sample, therewith avoiding biological variations. A limited number of *in vitro* studies onto cellular interactions with gradient surfaces have been done by us (Ruardy *et al.*, 1995; 1997) and others (Lee and Lee, 1993) showing, for instance, that a relatively high number of adhering cells can be found on the region of gradient surfaces with intermediate wettability (around 55 degrees), while the spread area of adhering cells usually reaches a

maximum on regions with advancing water contact angles around and below 55 degrees.

Flow chambers (Koslow *et al.*, 1986; Viggers *et al.*, 1980) have evolved into popular tools to study cellular interactions with biomaterials surfaces, primarily because they allow *in vitro* to mimic the natural flow and shear conditions, as occurring, for example, in an artificial vascular graft. We have developed a parallel plate flow chamber system, able to monitor the response of cells adhering to a biomaterial under exposure to flow with *in situ* observation of sequentially taken image series (Van Kooten *et al.*, 1991, 1992). In combination with the use of gradient surfaces, the system allows to monitor the position bound response of cells adhering on gradient surfaces under exposure to flow. Computer analysis of the images yields the position bound density of adhering cells, their shape and spread areas, as a measure of the strength of adhesion (Schakenraad *et al.*, 1986). Similarly, also the number of remaining cells after exposure to fluid flow or shear has been taken as an indirect measure of the strength of adhesion (Van Wachem *et al.*, 1985).

The aim of this study is to determine and compare the position bound behaviour of human umbilical cord endothelial cells (HUVEC) on three different types of wettability gradient surfaces during exposure to flow in a parallel plate flow chamber. All gradient surfaces employed will be characterized by advancing and receding water contact angles, measured by the Wilhelmy plate method and by their elemental surface composition measured employing scanning X-ray photoelectron spectroscopy (XPS).

Materials and methods

Preparation of gradient surfaces

Wettability gradients were prepared according to the diffusion technique described by Elwing *et al.* (1987) using two sizes of glass plates, namely 7.6 x 5.0 x 0.2 cm and 7.6 x 0.6 x 0.2 cm (l x w x h) purchased as microscope slides (Knittel, Germany). The smaller plates were used for characterization by the Wilhelmy plate method, while the larger plates were employed for flow chamber experiments. Cleaning of the glass was performed by storage in a strong detergent (2% RBS 35, Perstorp Analytical, Oud-beijerland, The Netherlands) for 16 h and subsequent rinsing in Millipore-Q filtered water, methanol and again Millipore-Q filtered water. After drying in a vacuum desiccator for 15 min samples were immediately placed in a beaker filled with xylene. A solution of dichlorodimethylsilane (DDS, 2.6×10^{-3} mol/l), dimethyloctadecylchlorosilane (DOCS, 1.9×10^{-2} mol/l) or (tridecafluor-1,1,2,2-tetrahydrooctyl)-1-dimethylchlorosilane (TFCS, 1.9×10^{-2} mol/l) in trichloroethylene was injected under the xylene phase through a drain in the beaker, allowing silane to diffuse into the xylene phase and react with the glass surface. After diffusion at room temperature, the solvents were removed through the drain of the beaker. The glass plates were then rinsed in trichloroethylene, methanol and Millipore-Q filtered water to remove unreacted silane from the surface. Gradient surfaces prepared on the larger glass plates were stored in methanol prior to flow chamber experiments, never longer than two weeks and sonicated for 7 min in methanol and rinsed in Millipore-Q filtered water prior to the assembly in the parallel plate flow chamber. Gradients prepared on the small plates were immediately characterized after preparation by the Wilhelmy plate method or by XPS after drying in a vacuum desiccator for 10 min.

All chemicals were purchased from Merck, Darmstadt, Germany) except for DOCS (Fluka Chemie AG, Buchs, Switzerland) and TFCS (ABCR, Karsruhe, Germany) and were of P.A. grade.

Wettability characterization by the Wilhelmy plate method

Advancing and receding water contact angles were recorded along the length of the gradients using the Wilhelmy plate method (Johnson and Dettre, 1969). Samples were fixed to a microbalance (Lauda tensiometer, Königshofen, Germany) and the force was continuously recorded while the plate was immersed into water at a constant speed of 27 mm/min. The contact angle θ was calculated as a function of the position along the length of the gradient from

$$F = p\gamma\cos\theta + (m - V\Delta\rho)g \qquad (1)$$

in which F is the force on the plate, p the perimeter of the slide, γ the liquid surface tension, m the mass of the plate, $\Delta\rho$ is the liquid-vapour density difference, g the acceleration of gravity and V the water volume displaced by the immersed part of the plate (Johnson and Dettre, 1969).

X-ray photoelectron spectroscopy

After preparation and cleaning, the samples were immediately placed in the pre-vacuum chamber of the XPS machine in order to prevent contamination of the surfaces. Spectra were obtained using an S-probe apparatus (Surface Science Instruments, Mountain View, California). The residual pressure in the spectrometer was approximately 10^{-7} Pa. An aluminum anode was used for X-ray production (10 kV, 22mA) at a spot size of 250 * 1000 μm^2. Spectra were taken at a high resolution of 50 eV and a photo emission angle of 35 degrees. Six positions were analysed with a distance of 10 mm between two subsequent positions. Relative atomic

percentages of silicon, carbon, oxygen and fluor were calculated from peak areas of Si_{2p}, C_{1s}, O_{1s} and F_{1s} using instrumental sensitivity factors as supplied by the manufacturer. Scanning XPS was done once per gradient surface.

Endothelial cell culturing and seeding

Human umbilical vein endothelial cells (HUVEC) were harvested from an umbilical vein essentially as described by Mulder *et al.* (1995). The primary culture (passage P0) and subsequently passaged cultures were grown in RPMI 1640 medium, supplemented with 100 U/ml penicillin, 100 μg/ml streptomycin, 2 mM L-glutamine (all from Gibco, Life Technologies, Breda, The Netherlands), 30 μg/ml endothelial cell growth factor (ECGF) and 10% pooled human serum (HPS) at 37°C in 5% CO_2 at 100% humidity. Cells were routinely grown on 80 cm^2 tissue culture quality plastic flasks (Nunclon delta), precoated with 0.2% gelatine in PBS (9.0 mM Na_2HPO_4, 1.3 mM KH_2PO_4, 140 mM NaCl, pH 7.0). At confluency, cells were subdivided (1:3) using trypsin-EDTA solution (Difco) in modified Puck's saline A up to three passages (P3). In order to minimize biological variations over longer periods of time, cells were initially harvested at P3, pooled in RPMI 1640 medium containing 10% DMSO and 45% HPS and subsequently subdivided over cryotubes and stored at -20°C (2 h), -80°C (24 h) before final storage in liquid nitrogen. Before each experiment with HUVEC cells, the contents of a cryotube was warmed up to room temperature. DMSO was removed by resuspension and centrifugation in DMSO free medium for two times. The HUVEC cells were brought into culture and harvested for the cellular experiments at P5. Cells were harvested by trypsinization using Trypsin-EDTA solution in modified Puck's saline A, suspended in 10% serum containing medium and seeded on the gradient surfaces positioned in the flow chamber to a density up to 200 cells/mm^2. Cells were allowed to adhere and spread for 3 h at 37°C. After 3 h flow was established with RPMI 1640 medium without any supplements.

The flow chamber system

The flow chamber system has been described in detail before (Van Kooten *et al.*, 1991). It contains three basic modules: the flow loop, the heating system, and the image analysis components. RPMI 1640 medium is pumped through the flow loop by a peristaltic pump (Watson-Marlow 503U with 8 mm inner diameter tubing) into a damping vessel. This vessel dampens the pulsations of the flow into a steady flow. Then the medium flows through a parallel plate flow chamber mounted on a phase contrast microscope stage. Medium is collected in a thermostatted double walled vessel. The flow chamber itself is heated to 37°C directly with four

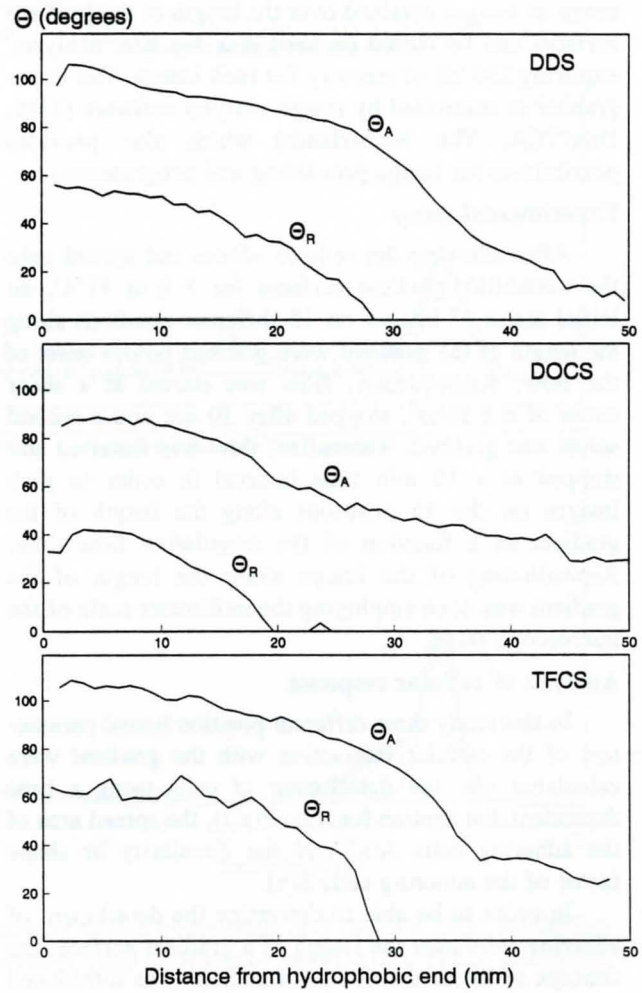

Figure 1: Advancing (θ_A) and receding (θ_R) water contact angles as a function of the distance from the hydrophobic end of a DDS, DOCS and TFCS-wettabiliy gradient on glass. Data represent the mean over two experimental runs with an average difference of 6 degrees.

---

power resistors (33 Ohm each), connected in parallel to a power supply (10 V) with feedback from a Pt-100 thermocouple situated in the downstream compartment of the flow chamber.

The image supplied by the microscope system (Olympus BH-2 with A10PL phase contrast objective and NFK 3.3x LD photo ocular) is registered with a CCD camera (type MO, High technology Holland BV) connected to the microscope with a MTV-3 (Olympus) connector and covers 0.28 mm^2 of the gradient surface. The signal from the CCD camera is digitized by a frame grabber (PCVision Plus, Imaging Technology Incorporated, USA) into an image consisting of 512 x 512 pixels, each pixel having 256 possible grey values. The

series of images obtained over the length of the gradient surfaces can be stored on hard disk for later analysis, requiring 256 kB of memory for each image. The frame grabber is controlled by image analysis software (TIM, Difa/TEA, The Netherlands) which also provides possibilities for image processing and programming.

Experimental setup

After allowing the cells to adhere and spread onto the wettability gradient surfaces for 3 h at 37°C, an initial series of images on 15 different positions along the length of the gradient were grabbed before onset of the flow. Subsequently, flow was started at a shear stress of 8.6 N/m^2, stopped after 10 sec and a second series was grabbed. Thereafter, flow was restarted and stopped at a 10 min time interval in order to grab images on the 15 positions along the length of the gradient as a function of the cumulative flow time. Repositioning of the image along the length of the gradient was done employing the millimeter scale of the microscope stage.

Analysis of cellular response

In this study three different position bound parameters of the cellular interaction with the gradient were calculated viz. the detachment of cells using a time dependent distribution function P(x,t), the spread area of the adhering cells A(x) and the circularity or shape factor of the adhering cells S(x).

In order to be able to determine the detachment of adhering cells over the length of a gradient surface, the concept of linear distribution functions was introduced (Ruardy *et al.*, 1995), in analogy to radial and angular pair distribution functions to analyze particle adhesion on collector surfaces (Sjollema and Busscher, 1990). The number of cells n in each image grabbed was counted and expressed as

$$P(x,t) = \frac{n(x,t)}{n_s(0)} \qquad (2)$$

in which P(x,t) is a time and position dependent linear distribution function, n(x,t) is the number of cells in an image at distance x from the hydrophobic end of the glass plate after a cumulative flow time t and $n_s(0)$ the mean number of cells per image over the length of the gradient surface within the series grabbed before onset of the flow. When seeded cells are initially homogeneously adhering over the length of the gradient surface, P(x,0) approximately equals unity. After cellular detachment, P(x,t) may become smaller than unity.

Prior to starting the flow, a number of randomly selected cells was outlined and the coordinates of the cells in each image were used to calculate a position bound spread area function $A_r(x)$ according to

$$A_r(x) = \frac{A(x)}{A_s} \qquad (3)$$

in which A(x) is the mean spread area of cells at distance x, A_s the mean spread area of cells over the length of the gradient surface within one series and $A_r(x)$ the relative spread area of the cells in an image at distance x.

Similarly, a position bound mean shape factor S(x) was calculated by averaging the shape factors of each individual adhering cell, defined as

$$S = \frac{1}{2(\pi A)^{1/2}} \qquad (4)$$

in which l and A are the perimeter and spread area of an individual cell, respectively. Since major detachment of adhering cells occurred on the hydrophobic end of the gradient surface almost immediately after the start of flow, position bound spread area functions and shape factors were only calculated for adhering cells prior to exposure to flow.

Results

Wettability characterization

Fig. 1 shows the advancing and receding water contact angles along the length of the DDS, DOCS and TFCS-wettability gradients on glass. On DDS-wettability gradients, advancing water contact angles changed gradually between 107 and 10 degrees. TFCS-wettability gradients were very similar to DDS-wettability gradients with a gradually changing advancing water contact angle between 107 and 23 degrees, while for DOCS-wettability gradients advancing water contact angles varied only between 88 and 30 degrees. Receding water contact angles were lower compared to advancing water contact angles along the whole length of the three wettability gradients with a typical contact angle hysteresis of about 45 degrees on the hydrophobic end of the gradients.

X-ray photoelectron spectroscopy

Fig. 2 shows narrow scans of the Si_{2p} and C_{1s} electron binding energies on the hydrophobic and hydrophilic ends of DDS and TFCS-wettability gradients on glass, respectively. On the hydrophobic end of the DDS-gradient, a relatively large amount of Si_{2p} electrons with lower binding energies, due to $Si\text{-}CH_3$ bonds and indicative of the presence of DDS, is observed compared to on the hydrophilic end. Similarly, on the hydrophobic end of the TFCS-wettability gradient, a large amount of C_{1s} electrons with higher binding

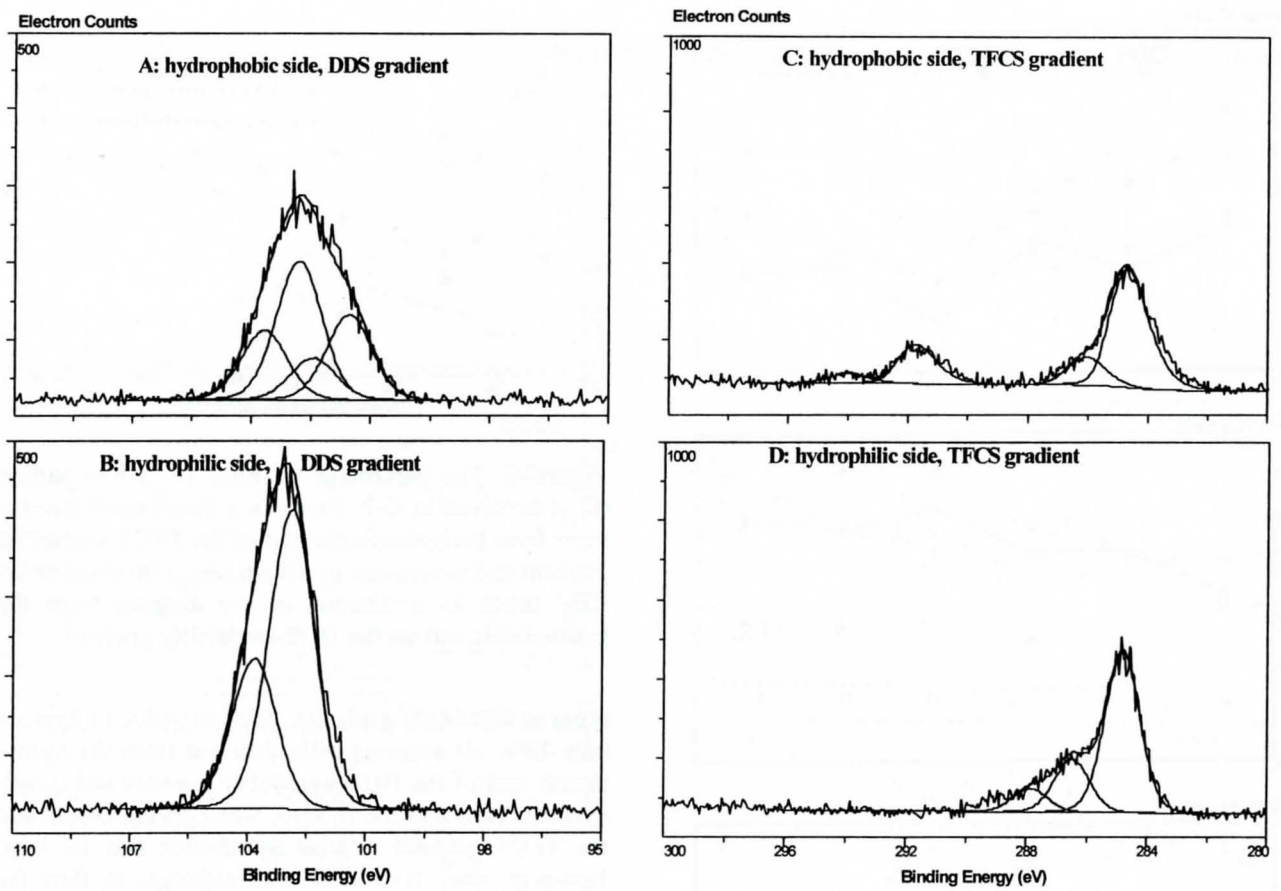

Figure 2. LEFT: Si_{2p} electron binding energies of the hydrophobic (A) and hydrophilic end (B) of a DDS-wettability gradient. RIGHT: C_{1s} electron binding energies of the hydrophobic (C) and hydrophilic end (D) of a TFCS-wettability gradient.

---

energy, due to C-F bonds and indicative of the presence of TFCS, was found.

Fig. 3 presents the atomic composition with respect to carbon, oxygen and silicon along the length of the wettability gradients. The atomic compositions of the hydrophilic ends of the gradients were approximately identical, with 20-30% C, 40-50% Si and 20-30% O.

A relatively high percentage of carbon on the hydrophilic end of the gradients was found and thought to be indicative of the presence of deposited carbonaceous contaminants from the air because only small amounts of carbon originating from silane are expected on the hydrophilic end of the gradients. On the hydrophobic end of the DDS-wettability gradient more carbon (27% compared to 20%) and less oxygen (42% compared to 50%) was found than on the hydrophilic end. The total amount of silicon measured was approximately 30%, independent of the position on the gradient. On the DOCS-wettability gradient, 40% of carbon was found on the hydrophobic end as compared to 28% on the hydrophilic end, accompanied by a simultaneous increase of the amount of oxygen from 41% to 50% on the hydrophilic end. Again, the percentage of silicon remained constant at 20%, independent of the position along the length of the gradient. On TFCS-wettability gradients, both the percentages of carbon and oxygen increased from approximately 30% to 38% towards the hydrophilic end, while the silicon percentage was 23% independent of position.

Fig. 4 presents the fluor percentage and the percentage of carbon in C-F bonds along the length of the TFCS-wettability gradient together with the percentage of silicon in $Si\text{-}CH_3$ bonds on the DDS-wettability gradient. The fluor content and the percentage of carbon bound to fluor were maximal on the hydrophobic end of the gradient and decreased from respectively 18 and 7% on the hydrophobic end to 0% on the hydrophilic end of the TFCS-wettability gradient. Similarly, silicon in $Si\text{-}CH_3$ bonds on the DDS-wettability gradient decreased from 12% on the hydrophobic end to 0% on the hydrophilic end.

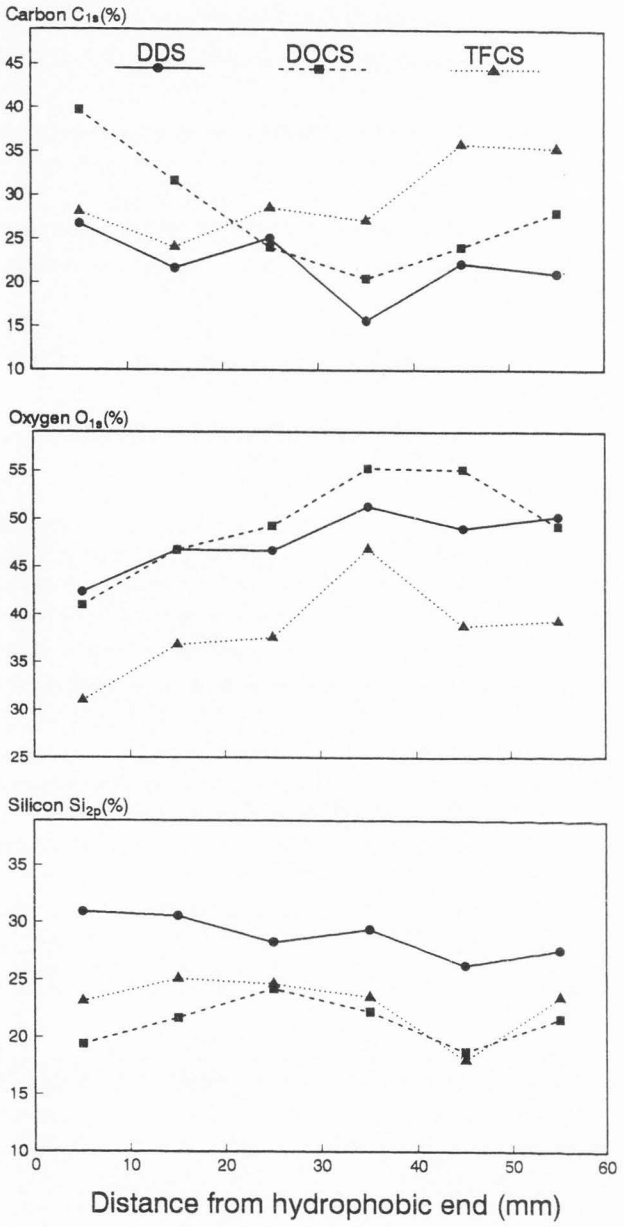

Figure 3. The percentage of carbon (C_{1s}), oxygen (O_{1s}) and silicon (Si_{2p}) as a function of the distance from the hydrophobic end on the DDS, DOCS and TFCS-wettability gradient.

Cellular interactions along the lengths of the gradients

Fig. 5 shows the distribution function P(x,t) of adhering endothelial cells along the lengths of the gradients after different periods of exposure to flow, which was always directed from the hydrophobic to the hydrophilic end of a gradient. Prior to exposure to flow, a homogeneous distribution of adhering cells was observed with P(x,t) hovering about unity for all three

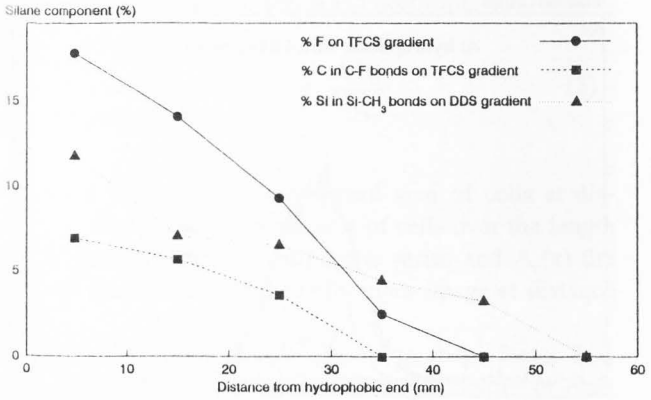

Figure 4. The percentage of fluor (F_{1s}) and carbon (C_{1s}) involved in C-F bonds as a function of the distance from the hydrophobic end on the TFCS-wettability gradient and percentage of silicon (Si_{2p}) involved in Si-CH_3 bonds as a function of the distance from the hydrophobic end on the DDS-wettability gradient.

---

types of wettability gradients. After exposure to flow for only 10 s, all adhering cells detached from the hydrophobic end of the DDS-wettability gradient and consequently P(x,t) reduced to zero, while on the DOCS and the TFCS gradient cellular detachment was far less. However, after 20 and 60 min exposure to flow the distribution function P(x,t) was significantly smaller than unity over the entire length of all three types of wettability gradients and appeared to be position dependent. On the DDS gradient, cells preferentially remained adhering around 40 mm and further away from the hydrophobic end, corresponding with an advancing water contact angle between 10 and 30 degrees. On the DOCS-wettability gradient, cells remained adhering in lower numbers over the entire length of the gradient surfaces, while on TFCS-wettability gradient, significant preferential adhesion occurred around 34 mm and above, corresponding with advancing water contact angles between 35 and 65 degrees.

Fig. 6 presents the position bound relative spread areas of human endothelial cells along the lengths of the DDS, DOCS and TFCS-wettability gradients. On the DDS-wettability gradient the relative spread area was smallest on the hydrophobic end (absolute spread area 660 μm^2) and gradually increased towards the hydrophilic end. In the case of the DOCS-wettability gradient, the position bound relative spread area was largest on the hydrophobic end (absolute spread area 2460 μm^2) and decreased gradually towards the hydrophilic end. On the TFCS-wettability gradient, position bound relative spread areas were minimal on the hydrophobic end of the gradient (absolute spread area 980 μm^2) and in-

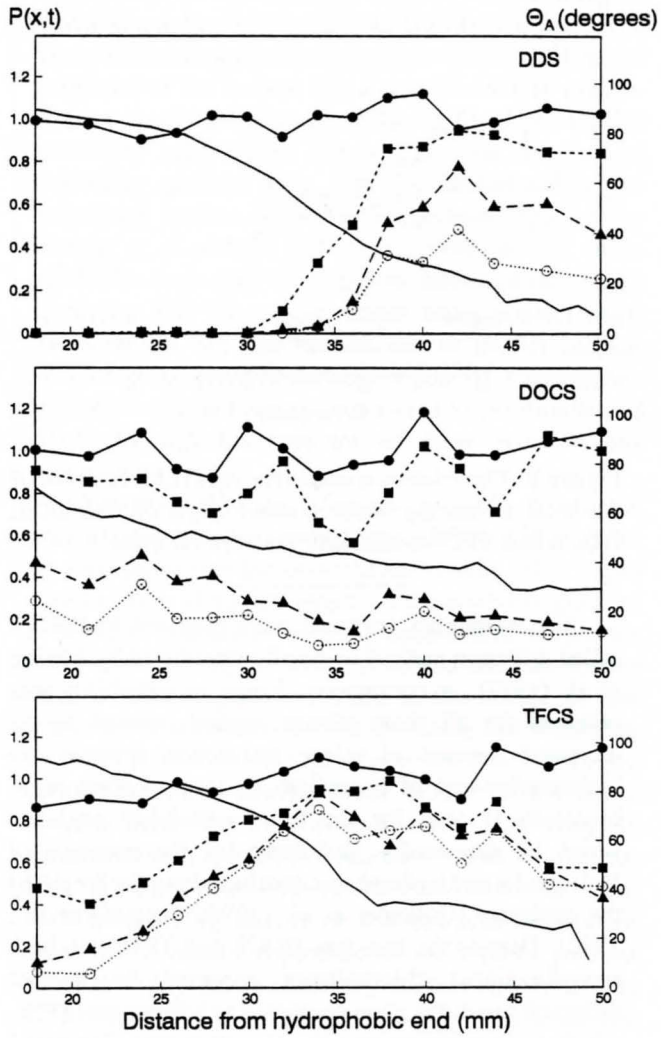

Figure 5. The distribution of adhering human endothelial cells P(x,t) along the length of the gradients (individual data points, left axis) and the advancing water contact angle θ_A (drawn line, right axis) as a function of the distance from the hydrophobic end of a DDS, DOCS and TFCS-wettability gradient surface on glass prior to (●) and after exposure to flow for 10 sec (■), 20 min (▲) and 60 min (○). Data represent the mean over two experiments comprising a total of 30 cells per data point prior to exposure to flow. The average difference between the two experiments for each data point is 0.2.

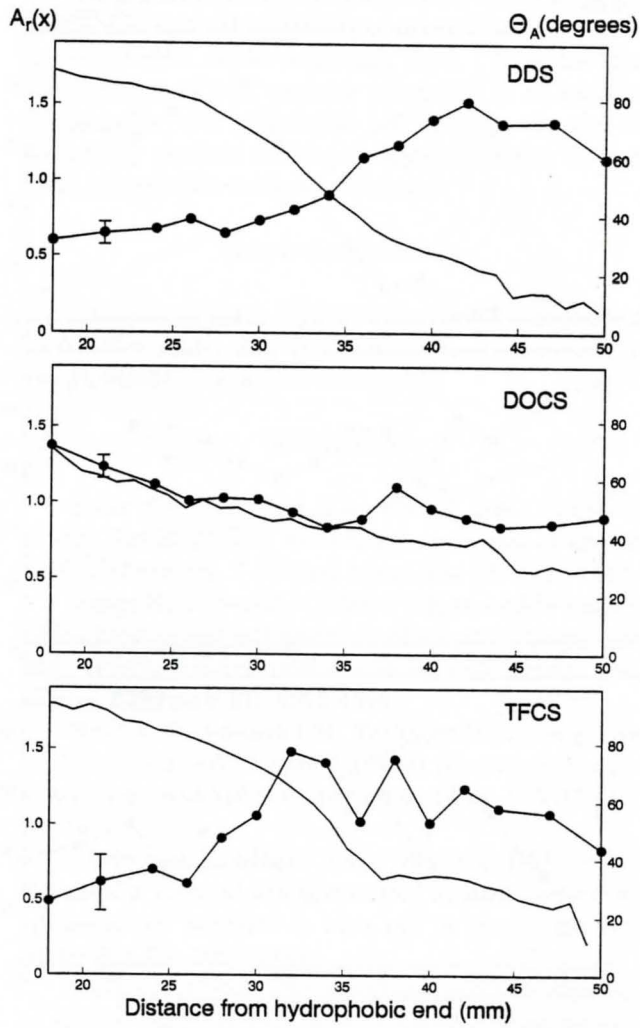

Figure 6. The relative spread area $A_r(x)$ of adhering human endothelial cells (individual data points, left axis) and the advancing water contact angle θ_A (drawn line, right axis) as a function of the distance from the hydrophobic end of a DDS, DOCS and TFCS wettability gradient on glass. Bars indicate the difference over two experiments comprising a total of 30 cells per data point.

---

creased towards a maximum on the transition region of the gradient (advancing water contact angles around 65 degrees).

Fig. 7 demonstrates the change in the position bound shape factor of adhering human endothelial cells occurring over the length of the DDS, DOCS and TFCS-wettability gradient. On DDS-wettability gradients the increase of the position bound shape factor is most pronounced and concurrent with the increase of the position bound spread area when going from the hydrophobic to the hydrophilic end of the gradient (compare Fig. 6).

Fig. 8 shows the relative spread area A_r as a function of the advancing water contact angle, measured on DDS, DOCS and TFCS-wettability gradients. On DDS-wettability gradients, cells adapted large spread areas on the hydrophilic end of the wettability spectrum around 25 degrees. On DOCS and TFCS-wettability

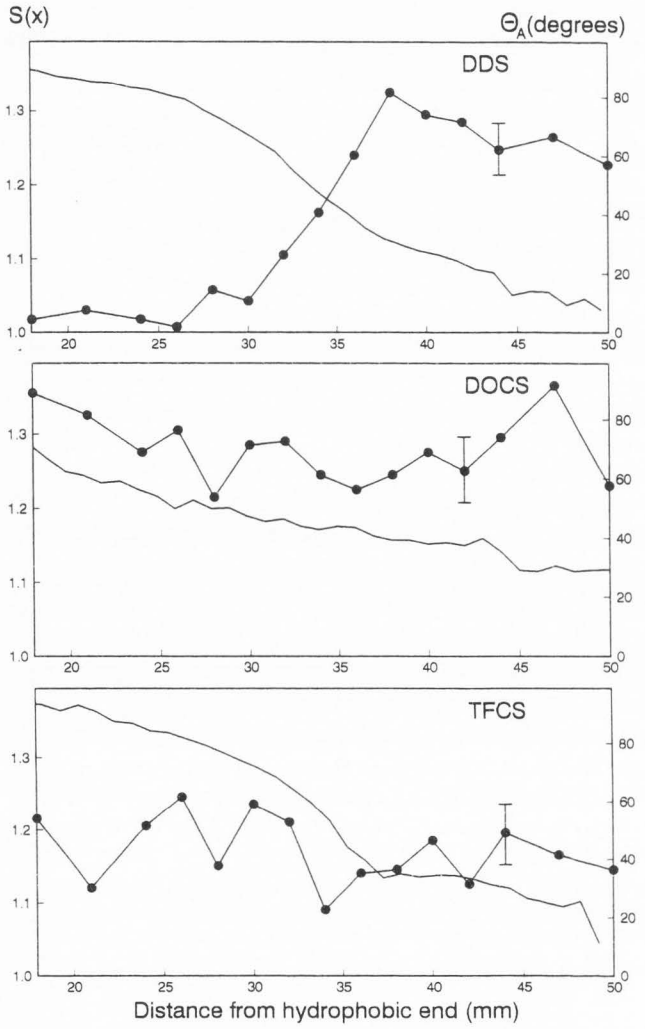

Figure 7. The shape factor S(x) of adhering human endothelial cells (individual data points, left axis) and the advancing water contact angle θ_A (drawn line, right axis) as a function of the distance from the hydrophobic end of a DDS, DOCS and TFCS wettability gradient on glass. Bars indicate the difference over two experiments comprising a total of 30 cells per data point.

---

gradients, cell spreading was optimal around 65 degrees.

Discussion

In this paper we studied the position bound shape, spreading and detachment of adhering human endothelial cells on DDS, DOCS and TFCS-wettability gradients during exposure to flow in a parallel plate flow chamber in the presence of serum proteins. The wettability gradients were characterized by water contact angle measurements and X-ray photoelectron spectroscopy.

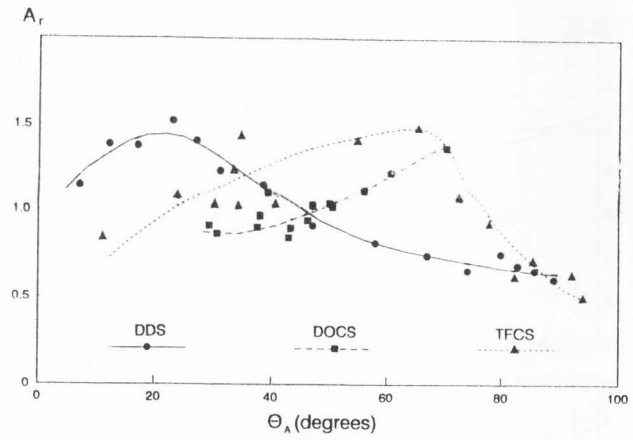

Figure 8. The relative spread area $A_r(x)$ as a function of the local advancing water contact angle on the DDS, DOCS and TFCS-wettability gradient on glass.

The wettability gradients were prepared by the so-called diffusion method originally introduced by Elwing *et al.* (1987). A continuous change in wettability was obtained for all three silanes applied, caused by an increased amount of silane interaction towards the hydrophobic end of a gradient. A large contact angle hysteresis is seen for the three wettability gradients which is, supposedly, indicative for the presence of hydrophilic and hydrophobic patches along the length of the gradients (Gölander *et al.*, 1990; Tengvall *et al.*, 1992). Despite the fact that DOCS and TFCS are both monofunctional chlorosilanes expected to interact differently with the glass compared to bifunctional DDS, which is in addition capable to polymerize (Hair and Hertl, 1969), the wettability of monofunctionally coupled TFCS and bifunctionally coupled DDS appears similar. Advancing water contact angles were lower on the hydrophobic end of DOCS-gradients (88 degrees) compared to the TFCS and DDS-gradients (107 degrees) probably because of steric hindrance amongst the relatively long DOCS-chains avoiding a complete coverage of the glass. The hydrophilic ends of the three wettability gradients were contaminated by carbonaceous components, as can be concluded from the water contact angle hysteresis and the relative large amounts of carbon (20% to 30%) measured by XPS.

In the present paper, the interaction of human endothelial cells on the wettability gradients took place in the presence of serum proteins, forming a conditioning film over the surfaces. Wettability gradient surfaces have been used frequently to study the adsorption of single proteins (Elwing *et al.*, 1987; Gölander and Pitt, 1990) or of selected proteins from protein mixtures like serum (Warkentin *et al.*, 1994), concluding that the

composition of an adsorbed protein film is position bound along the length of a wettability gradient. The nature of the deposited protein film which transfers the properties of the surface into a specific cellular interaction is not only different along the length of one type of wettability gradient but depends also on the type of wettability gradient (see Fig. 8). Unfortunately the underlying surface properties like chain length (Van Damme *et al.*, 1991; Pitt *et al.*, 1988) and/or chain orientation have their own specific influence on protein adsorption and the use of simple water contact angle measurements are thus insufficient to predict cellular interactions on gradient surfaces in general. Consequently, cellular interactions are controlled by position bound effects through the presence of these proteinaceous conditioning films.

Assuming that the adhesive strength of cells is proportional with their spread area (Hubbe, 1981), it can be anticipated that the distribution of cells, after exposure to flow, along the length of a wettability gradient (Fig. 5) is concurrent with the spread area before the onset of flow (Fig. 6) which is indeed the case for the three wettability gradients tested in this study. At first glance the relation between cell spreading and wettability seems to depend on the type of gradient used but a clear picture cannot be derived easily from Fig. 6 because distance from the hydrophobic end is not uniquely connected with the local wettability on each gradient. Fig. 8 shows the relation between wettability and cellular spreading and shows that the relation between these two is indeed dependent on the type of gradient used. Probably this is caused by the fact that wettability is a macroscopic property reflecting the combined influence of the number of silane patches and their size, the molecular orientation within these patches and the chemistry of the specific end group. On homogeneously silanized surfaces, it has been demonstrated that in the early stages of silane coupling, like towards the hydrophilic ends of our gradients, the number and size of silane patches (Flinn *et al.*, 1994; Banga and Yarwood, 1995) as well as the molecular orientation within patches (Rabinovitch and Yoon, 1994) are randomly distributed to maximize entropy. On the hydrophobic end of these gradients, entropy loss by deformation (or stretching) of the chains may be compensated by the binding energy gained in the adsorption and clustering process as suggested by Hähner *et al.* (1993) for alkanethiol treated gold surfaces. Obviously, the above considerations do not hold the short chain DDS-gradients. On the hydrophobic ends of these gradient, adsorption will be not so much entropy driven but much more enthalpy driven.

DDS, DOCS and TFCS-wettability gradient surfaces demonstrated different position bound endothelial cell adhesion and detachment behaviour along their lengths. For each specific chemical functionality constituting the gradient an optimal wettability could be found for which adhering cells could withstand flow. Thus for the development of e.g. vascular prostheses to be used in combination with endothelial cell seeding, the use of wettability gradient surfaces is highly effective to find ideal biomaterials surface properties.

Acknowledgements

The authors thank Joop de Vries for his contribution to the XPS study. This research has been supported by the ISP research grant IV-1 S91.003.

References

Baier RE, DePalma VA, Coupil DW, Cohen E (1985) Human platelet spreading on substrata of known surface chemistry. J Biomed Mater Res **19**: 1157-1167.

Banga R, Yarwood J (1995) FTIR and AFM studies of the kinetics and self-assembly of alkyltrichlorosilanes and (Perfluoroalkyl)trichlorosilanes onto glass and silicon. Langmuir **11**: 4393-4399.

Bruil A, Brenneisen LM, Terlingen JGA, Beugeling T, Van Aken WG, Feijen J (1994) *In vitro* leukocyte adhesion to modified polyurethane surfaces. J Coll Interf Sci **165**: 72-81.

Chehroudi B, Gould TRL, Brunette DM (1989) Effect of a grooved titanium-coated implant surface on epithelial cell behavior *in vitro* and *in vivo*. J Biomed Mater Res **23**: 1067-1085.

Davies JE (1988) The importance and measurement of surface charge species in cell behaviour at the biomaterial interface. In: Surface characterization of Biomaterials (Ratner BD, ed) Elsevier Science Publishers, Amsterdam, pp 219-234.

Elwing H, Welin S, Askendahl A, Nilsson U, Lundström I (1987) A wettability gradient method for studies of macromolecular interactions at the liquid/solid interface. J Coll Interf Sci **119**: 203-210.

Flinn DH, Guzonas DA, Yoon RH (1994) Characterization of silica surfaces hydrophobized by octadecyltrichlorosilane. Coll Surf A: Physicochem Eng Asp **87**: 163-176.

Groth T, Altankov G, Klosz K (1994) Adhesion of human peripheral blood lymphocytes is dependent on surface wettability and protein preadsorption. Biomaterials **15**: 423-428.

Gölander CG, Pitt WG (1990) Characterization of hydrophobicity gradients by means of radio frequency plasma discharge. Biomaterials **11**: 32-35.

Gölander CG, Lin YS, Hlady V, Andrade JD (1990) Wetting and plasma-protein adsorption studies using surfaces with a hydrophobicity gradient. Coll Surf

49: 289-302.

Hair ML, Hertl W (1969) Reactions of chlorosilanes with silica surfaces. J Phys Chem **73**: 2372-2378.

Hubbe MA (1981) Adhesion and detachment of biological cells *in vitro*. Prog Surf Sci **11**: 65-138.

Hähner G, Wöll Ch, Buck M, Grunze M (1993) Investigation of intermediate steps in the self-assembly of n-alkanethiols on gold surfaces by soft X-ray spectroscopy. Langmuir **9**: 1955-1959.

Johnson RE, Dettre RH (1969) Wettability and contact angles. In: Surface and Colloid Science, Vol 2 (E. Matijevic, ed) Wiley Interscience, New York, pp 85-154.

Kishida A, Iwata H, Tamada Y, Ikada Y (1991) Cell behaviour on polymer surfaces grafted with non-ionic and ionic monomers. Biomaterials **12**: 786-792.

Koslow AR, Stromberg RR, Friedman LI, Lutz RJ, Hilbert SL, Schuster P (1986) A flow system for the study of shear forces upon cultured endothelial cells. J Biomech Eng **108**: 338-341.

Lee JH, Lee HB (1993) A wettability gradient as a tool to study protein adsorption and cell adhesion on polymer surfaces. J Biomater Sci Polym Edn **4**: 467-481.

Mulder AB, Blom NR, Smit JW, Ruiters MHJ, Van der Meer J, Halie MR, Bom VJJ (1995) Basal tissue factor expression in endothelial cell cultures is caused by contaminating smooth muscle cells. Reduction by using chymotrypsin instead of collagenase. Thromb Res **80**: 399-411.

Pitt WG, Grasel TG, Cooper SL (1988) Albumin adsorption on alkyl chain derivatized polyurethanes: II The effect of alkyl chain length. Biomaterials **9**: 36-46.

Rabinovitch YI, Yoon RH (1994) Use of atomic force microscope for the measurements of hydrophobic forces between silanated silica plate and glass sphere. Langmuir **10**: 1903-1909.

Ruardy TG, Schakenraad JM, Van der Mei HC, Busscher HJ (1995) Adhesion and spreading of human skin fibroblasts on physicochemically characterized gradient surfaces. J Biomed Mater Res **29**: 1415-1423.

Ruardy TG, Moorlag HE, Schakenraad JM, Van der Meer J, Van der Mei HC, Busscher HJ (1997) The interaction of human endothelial cells with chemical gradient surfaces during exposure to flow. J Adh Sci Technol, in press.

Schakenraad JM, Busscher HJ, Wildevuur CRH, Arends J (1986) The influence of substratum free energy on growth and spreading of human skin fibroblasts in the presence and absence of serum proteins. J Biomed Mater Res **20**: 773-784.

Schakenraad JM, Kuit JH, Arends J, Busscher HJ, Feijen J, Wildevuur CRH (1987) *In vivo* quantification of cell-polymer interactions. Biomaterials **8**: 207-210.

Sjollema J, Busscher HJ (1990) Deposition of polystyrene latex particles in a parallel plate flow cell-Pair distribution functions between deposited particles. Coll Surf **47**: 337-352.

Steele JG, Johnson G, Norris WD, Underwood PA (1991) Adhesion and growth of cultured human endothelial cells on perfluorosulphonate: role of vitronectin and fibronectin in cell attachment. Biomaterials **12**: 531-539.

Tengvall P, Olsson L, Wälivaara B, Askendal A, Lundström I, Elwing H (1992) Deposition of antisera onto methyl gradients after immersion in human plasma: An *in vitro* study. In: Biomaterials-Tissue Interfaces, Advances in Biomaterials Vol 10 (Doherty P, ed) Elsevier Science Publishers, Amsterdam, pp 511-519.

Van Damme HS, Beugeling T, Ratering MT, Feijen J (1991) Protein adsorption from plasma onto poly (n-alkyl methacrylate) surfaces. J Biomater Sci Polym Ed **3**: 69-84.

Van Kooten TG, Schakenraad JM, Van der Mei HC, Busscher HJ (1991) Detachment of human fibroblasts from FEP-Teflon surfaces. Cells and Materials **1**: 307-316.

Van Kooten TG, Schakenraad JM, Van der Mei HC, Busscher HJ (1992) Cellular responses to environmental stimuli. Influence of fluid shear and substratum hydrophobicity on human fibroblast adhesion. Biofouling **5**: 239-246.

Van Wachem PB, Beugeling T, Feijen J, Bantjes A, Detmers JP, Van Aken WG (1985) Interaction of cultured human endothelial cells with polymeric surfaces of different wettabilities. Biomaterials **6**: 403-408.

Viggers RF, Wechezak AR, Sauvage LR (1980) An apparatus to study the response of cultured endothelium to shear stress. J Coll Interf Sci **76**: 305-314.

Warkentin P, Wälivaara B, Lundström I, Tengvall P (1994) Differential surface binding of albumin, immunoglobulin G and fibrinogen. Biomaterials **15**: 786-795.

Discussion with Reviewers

A. Underwood: You have mentioned that cellular interaction with the surface is controlled by the nature of the proteinaceous conditioning film. Have you any experiments planned to determine the concentration and confirmation of particular cell-adhesive plasma proteins along your wettability gradients, or to look at adhesion and flow studies in media containing selected specific proteins only.

Authors: At present, we have no such experiments planned.

H. Elwing: In Fig. 1 you present the wettability distribution on gradients made by DDS, DOCS and TFCS.

The resulting wettability gradients have about the same length (around 30 mm) for all three reagents. The DDS molecule is much smaller (more than ten times?) than DOCS and TFCS. It would have been expected that gradients of wettability distribution made by DDS should have been much longer providing that the similar diffusion time was used. Have you any explanation to this unexpected phenomenon?
Authors: The diffusion length is proportional with the square root of the diffusion coefficient. The diffusion coefficient varies with the reciprocal of the volume to the power 1/3. All and all there is not a tremendous dependence of the diffusion length on molecular size. Besides we made adjustments to the diffusion time to obtain the gradients as presented.

H. Elwing: I understand that the TFCS molecule contains long chains of fluorocarbons and that the carbon is located closer to the Si atom. If the molecule is attached with its (ordered) fluorocarbon chains upwards you might see a higher ratio of F/C with XPS at the surface sensitive mode (low angle) compared to a bulk sensitive mode (high angle). Have you thought of the possibility of using XPS in this way to assess the possible binding structure of TFCS.
Authors: We have thought about doing this, but the amount of valuable XPS time involved is enormous. For this reason, these experiments remain to be done.

H. Elwing: The conclusions in the paper that the short length DDS molecule is unfavourable for cell interactions compared to long chain groups is very interesting. Does this mean that you consider the wettability parameter is of minor analytical interest at surfaces were cells should be grown?
Authors: We do not wish to say that wettability is of minor interest for cell growth, but rather that cell growth is determined by an interplay of, amongst others, the specific chemistry, molecular length (mobility) and wettability of the substratum surface.

H. Elwing: What remains when cells are detached? Do the cells leave adsorbing molecules behind?
Authors: We do not know.

H.B. Lee: Why were smaller plates used for characterization by the Wilhelmy plate method instead of the plates used for cell interactions?
Authors: The larger plates were too heavy for our balance.

H.B. Lee: How was the cleanliness of the glass surfaces verified?
Authors: Glass plates were consider clean when they had a zero degree advancing water contact angles immediately after cleaning.

H.B. Lee: The authors indicated the presence of deposited carbonaceous contaminants from air on the hydrophilic end of the gradients from their water contact angle and XPS data. Why is only the hydrophilic end contaminated instead of the whole range of the gradient? If some range of the gradient is contaminated, how can the authors correlate the interaction of cells with the pure, silanized surfaces, not carbonaceous surfaces?
Authors: Hydrophilic surfaces become more easily contaminated than hydrophobic surfaces, due to their high surface free energies. We do not see how this (minor!) carbonaceous contamination on the hydrophilic end would interfere with our interpretation.

H.B. Lee: The authors sonicated the silane-deposited glass plates prior to the assembly in the parallel flow chamber. Why? Does the sonication step not affect silanes deposited on the glass surfaces?
Authors: Sonication reduces the carbon contamination and therewith restores the authentic gradient without affecting the silane, which is co-valently coupled to the glass.

H.B. Lee: In Fig. 3 from XPS analysis, why exist the minimum C_{1S} values for DDS and DOCS gradient surfaces and the maximum O_{1S} value for TFCS gradient surfaces on the positions between 30-40 mm?
Authors: We do not know why these minima and maxima arise where they do, but this must be due to an increased coverage of the surface by carbon containing silanes versus a decreased exposure of oxygen in glass (SiO_2).